Texas A&M University Engineering

July 27, 2023

N.K. Anand

Professor, Department of Mechanical Engineering

Texas A&M University

Experimental Investigations of HTGR Fission Product Transport in Separate-effect Test Facilities Under Prototypical Conditions for Depressurization and Water-Ingress Accidents

N.K. Anand[1], Y.A. Hassan[1], P. Sabharwall[2], H. Choi[3], E. Mulder[4], R. Chavez[1]

1.Texas A&M University 2. Idaho National Lab 3. General Atomics 4. X-Energy

DOE ART Gas-Cooled Reactor (GCR) Review Meeting

Virtual Meeting

July 25 – 27, 2023

ART Advanced Reactor Technologies

Overview & Objectives

Overview

1. Introduction
2. High pressure, high temperature experimental facility
3. Atmospheric P/T deposition experiments
4. Model development, numerical validation, scaling, & parametric study
5. Project timeline

Objectives

- Perform experiments to obtain plate-out , lift-off and wash-off of dust facilitated fission product transport from scaled reactor components at both scaled and representative conditions using existing experimental facilities.
- Implement models and perform simulations using the experimental conditions and match experimental data.
- Perform MELCOR simulations to compare with experiments and CFD.
- Derive numerical models and correlations from the generated data.

Introduction

- Analytical tools used to predict and determine source term transport currently suffer from large degrees of uncertainty for specific transport modes.
- It is known that certain FPs have a propensity to sorb onto the surfaces of particulates ("dust").
- Recirculation, deposition, and resuspension of FP sorbed dust is of concern to due its ability for release upon a LOCA.
- Plateout considers the mechanism in which condensable FPs deposit onto helium-wetted surfaces.
- Whether the FPs are primarily transported as an atomic species mixed into the coolant, or sorbed onto dust, liftoff accounts for the all transport methods which capture the resuspension of FP release upon a LOCA.
- Washoff concerns the entrance of water into the primary circuit which then becomes the transport mode of FPs sorbed to metallic surfaces or dust.

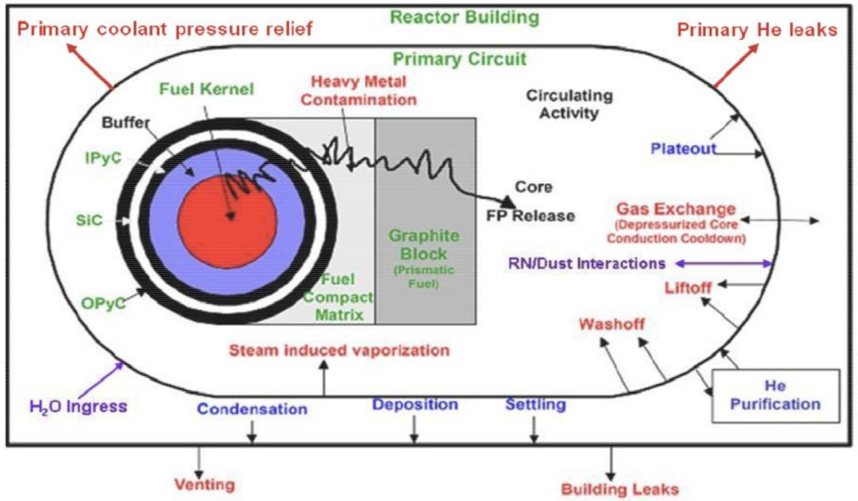

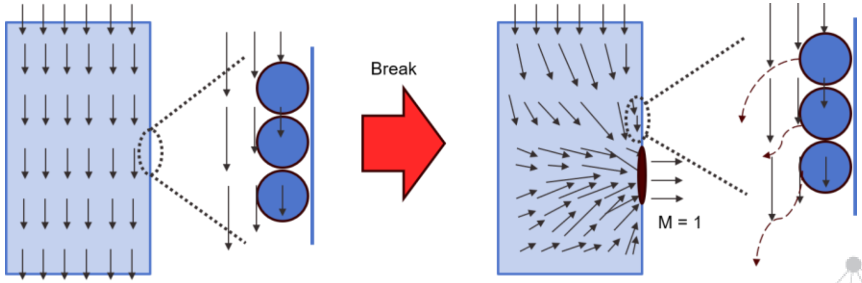

High Pressure High Temperature (HPHT) Experimental Facility

- Dust deposition & resuspension experiments under Normal Operating Conditions (NOC) and Loss of Coolant Accidents (LOCA).
- Improve Plate-out, Lift-off, & Wash-off (PLW) predictive models
- ASME rated to 1000°F, 1000 PSI

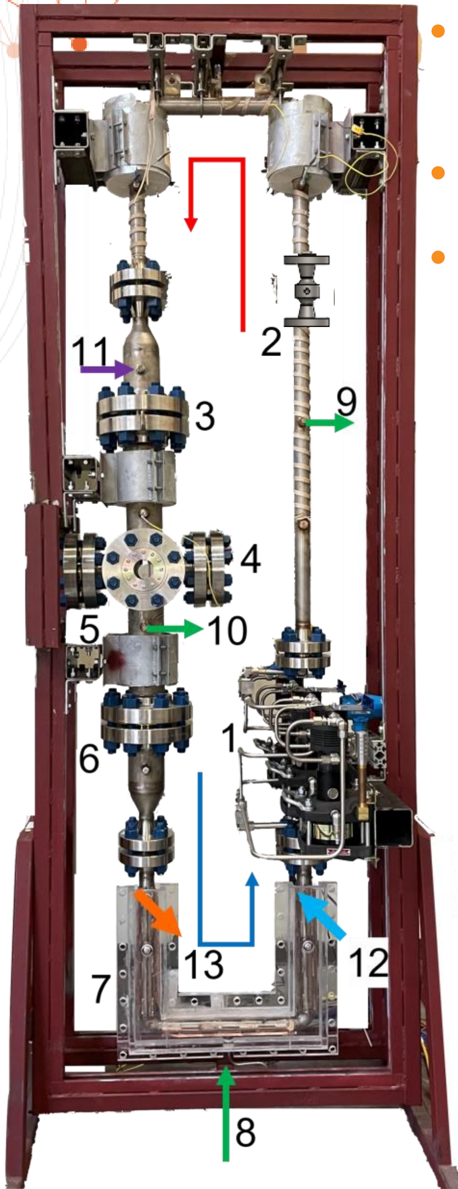

1. Gas Boosters
2. Orifice Flowmeter
3. Flow Conditioner
4. Test Article Mounting/Feedthroughs
5. Quartz Sight Glass Windows for Imaging
6. In-Line Filtration
7. Cooling Jacket
8. Gas Filling
9. Pressure Control Valve (PID)
10. Rapid Depressurization Valve
11. Liquid/Solid Aerosol Injection

12.-13. Cooling Jacket Water Inlet/Outlet

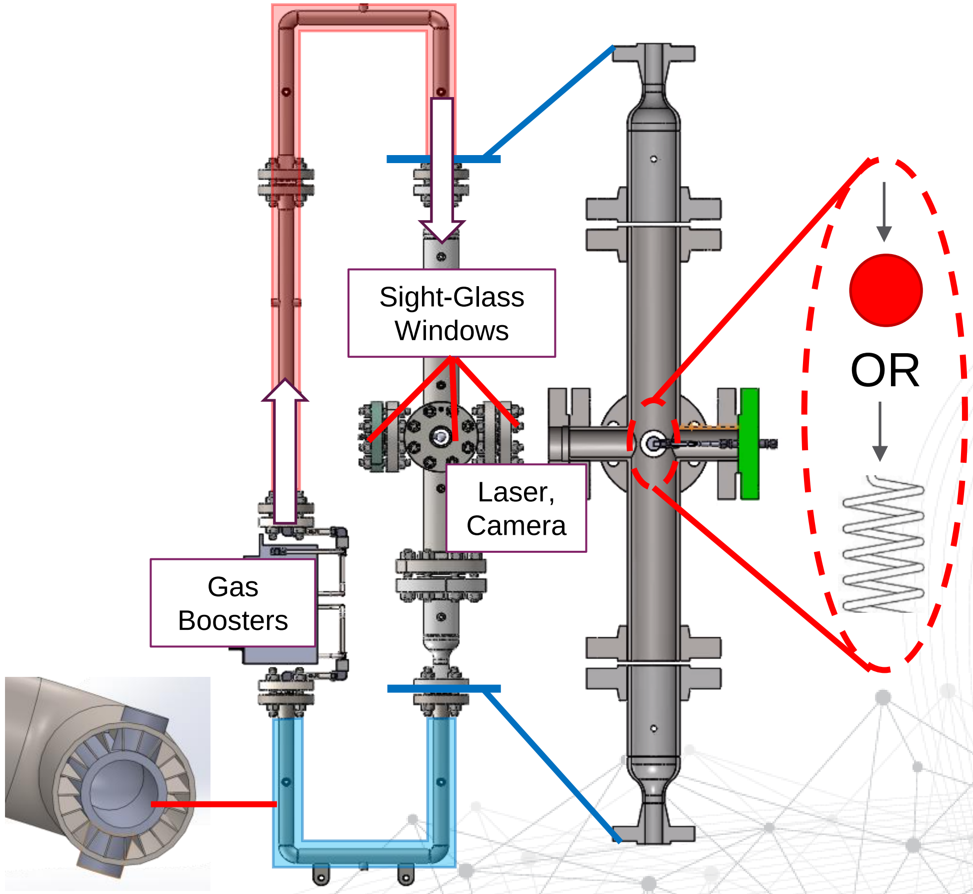

High Pressure High Temperature (HPHT) Experimental Facility

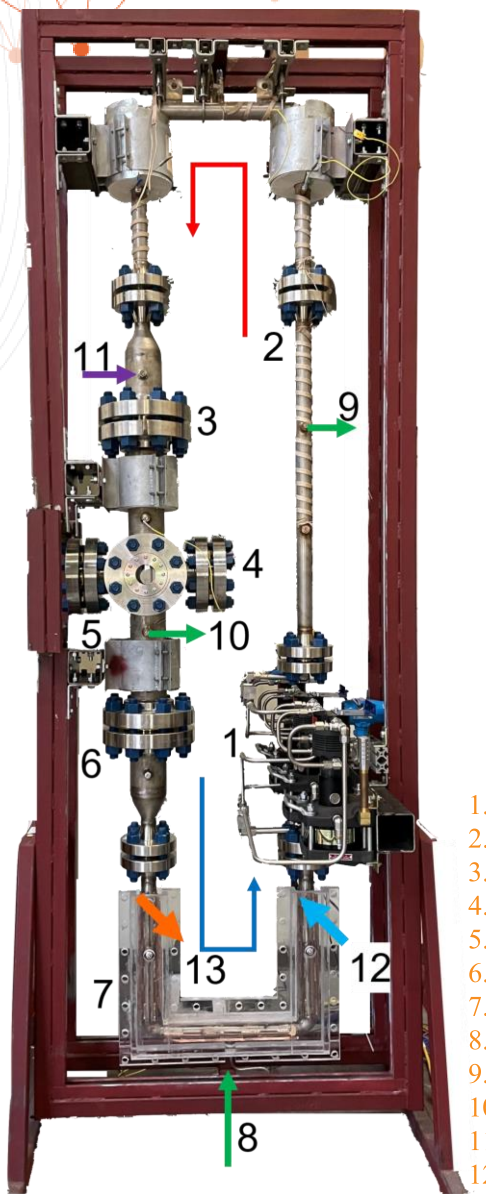

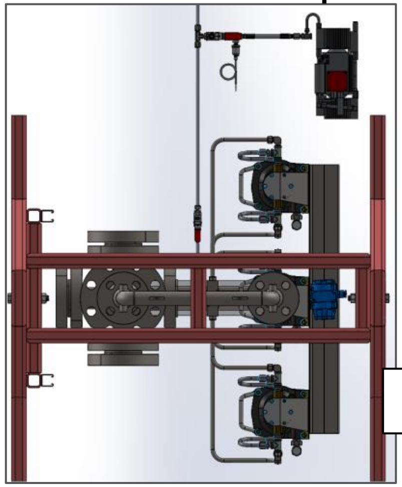

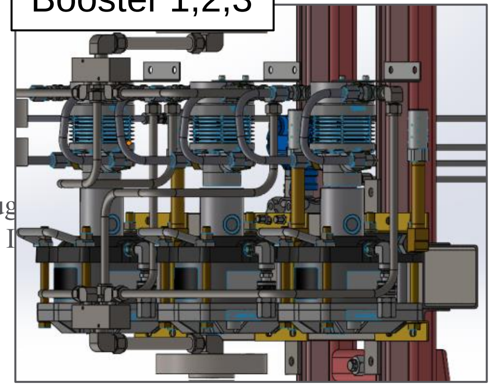

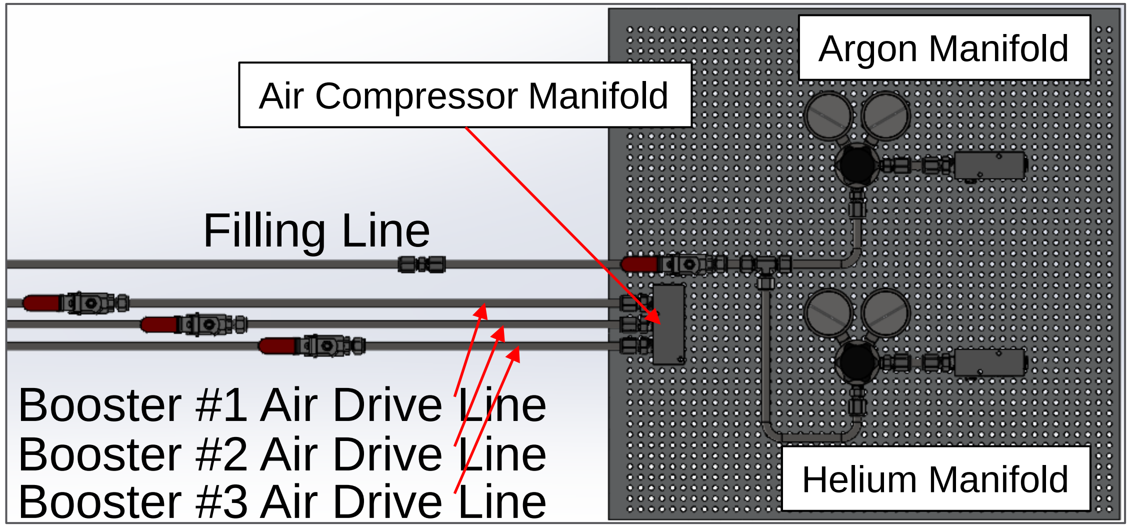

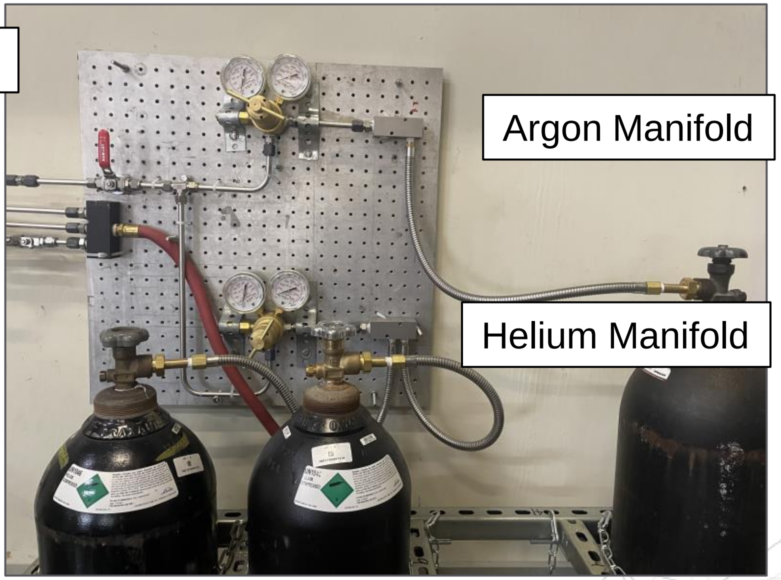

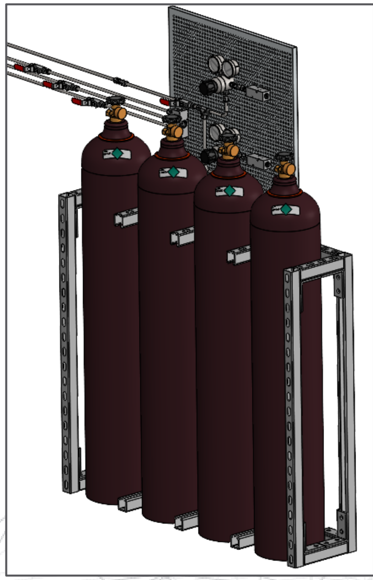

1. Gas Boosters
2. Orifice Flowmeter
3. Flow Conditioner
4. Test Article Mounting/Feedthroug
5. Quartz Sight Glass Windows for I
6. In-Line Filtration
7. Cooling Jacket
8. Gas Filling
9. Pressure Control Valve (PID)
10. Rapid Depressurization Valve
11. Liquid/Solid Aerosol Injection

12.-13. Cooling Jacket Water Inlet/Outlet

High Pressure High Temperature (HPHT) Experimental Facility

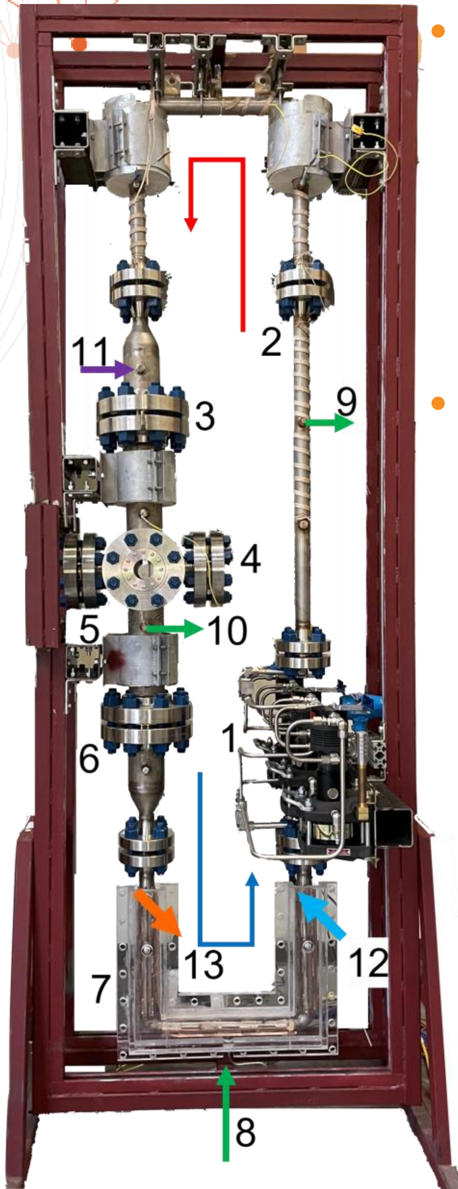

- Single Sphere Test Article for Non-Isothermal Case
- Joule Heating up to 2,000W Heating

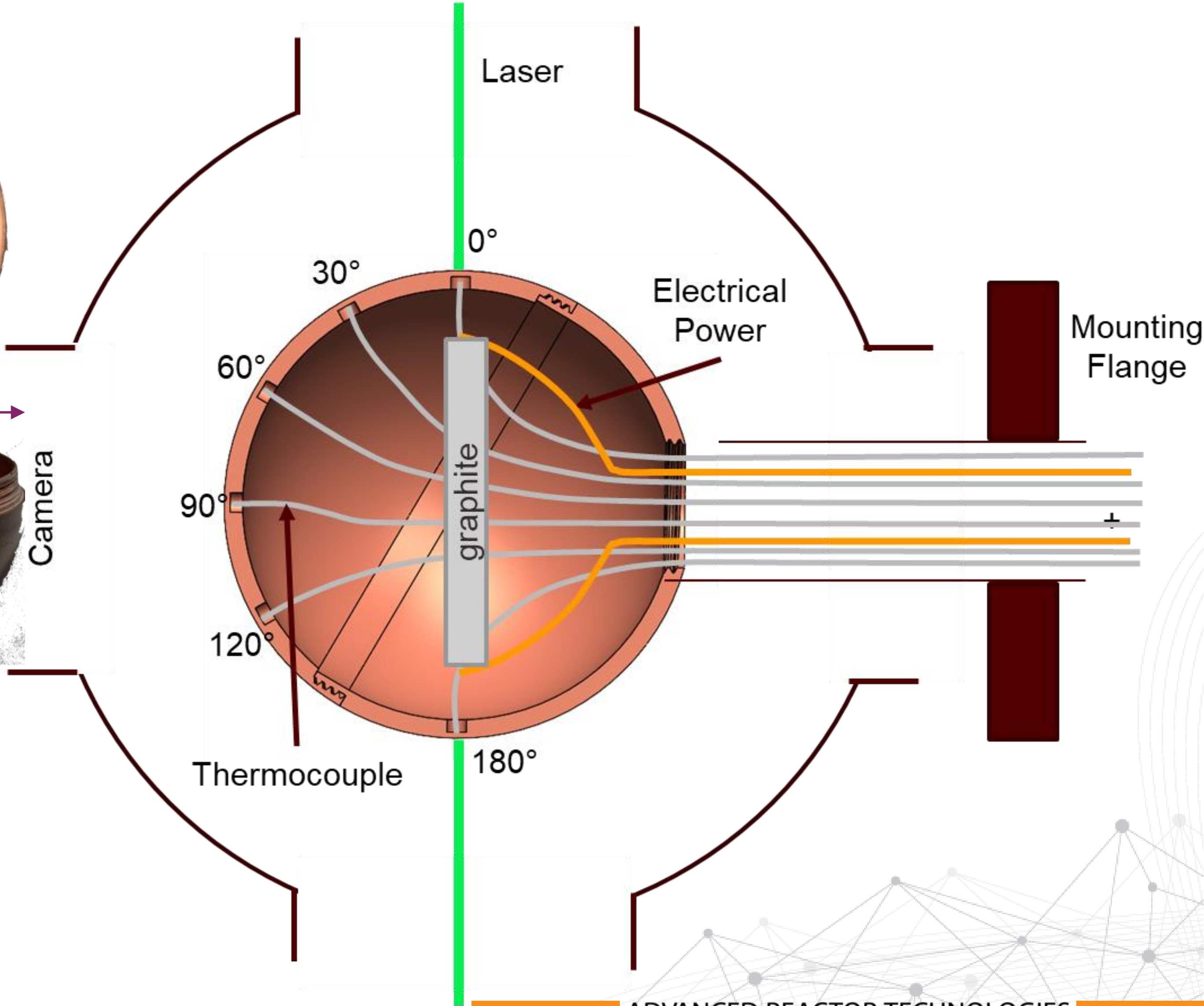

1. Gas Boosters
2. Orifice Flowmeter
3. Flow Conditioner
4. Test Article Mounting/Feedthroughs
5. Quartz Sight Glass Windows for Imag
6. In-Line Filtration
7. Cooling Jacket
8. Gas Filling
9. Pressure Control Valve (PID)
10. Rapid Depressurization Valve
11. Liquid/Solid Aerosol Injection

12.-13. Cooling Jacket Water Inlet/Outle

High Pressure High Temperature (HPHT) Experimental Facility

TEXAS A&M UNIVERSITY Engineering

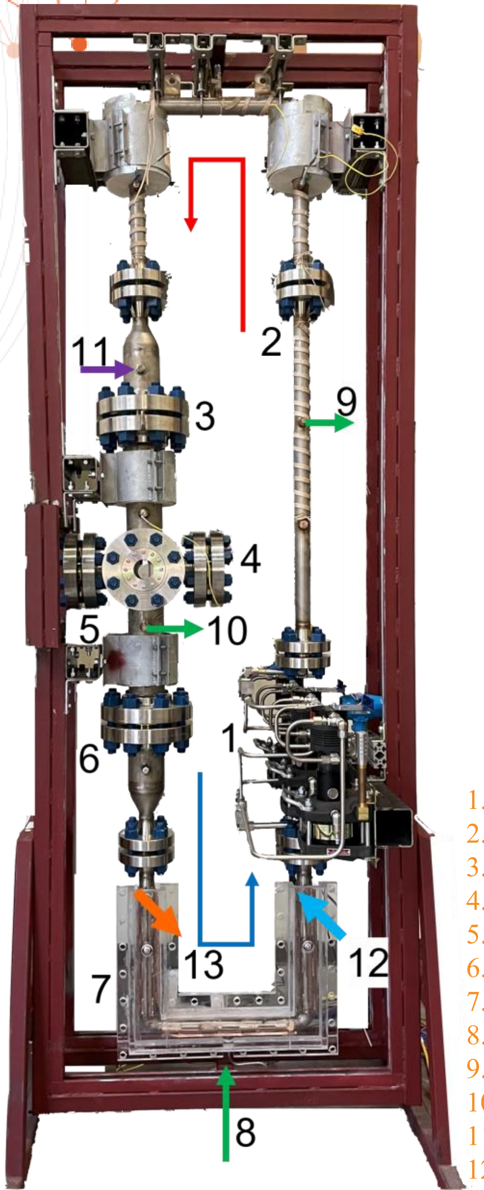

1. Gas Boosters
2. Orifice Flowmeter
3. Flow Conditioner
4. Test Article Mounting/Feedthroughs
5. Quartz Sight Glass Windows for Imaging
6. In-Line Filtration
7. Cooling Jacket
8. Gas Filling
9. Pressure Control Valve (PID)
10. Rapid Depressurization Valve
11. Liquid/Solid Aerosol Injection
12.-13. Cooling Jacket Water Inlet/Outlet

Solid Aerosol Generator

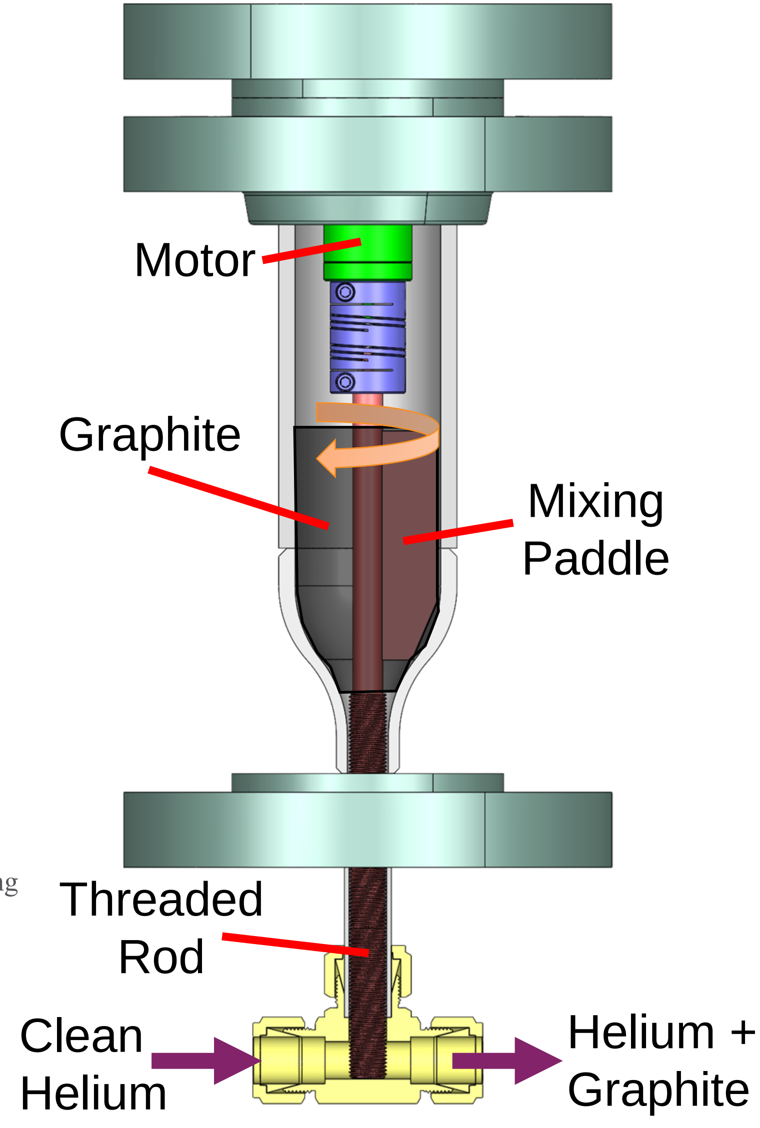

Liquid Aerosol Generator

Selection Criteria	
Re #	16,780
Stk #	0.02887
$\dot{m}_{water,max}$	1.79 LPH
$D_{drop,\ max}$	12μm

Flow Factor	Pressure (Bar)		
	25	30	40
	Capacity (Lph)		
15	1,70	1,83	2,11
20	2,38	2,61	2,99
30	3,86	4,22	4,86
40	5,22	5,72	6,56
50	6,58	7,17	8,31

Code	ø Min. Droplet	ø Max. Droplet	ø Med. Droplet
IIA15R1	6.60 μm	26.45 μm	11.0 μm
IIA20R1	6.69 μm	28.29 μm	11.0 μm
IIA30R1	7.18 μm	32.21 μm	12.0 μm
IIA40R1	7.42 μm	34.68 μm	12.0 μm
IIA50R1	7.49 μm	37.52 μm	12.0 μm

High Pressure High Temperature (HPHT) Experimental Facility

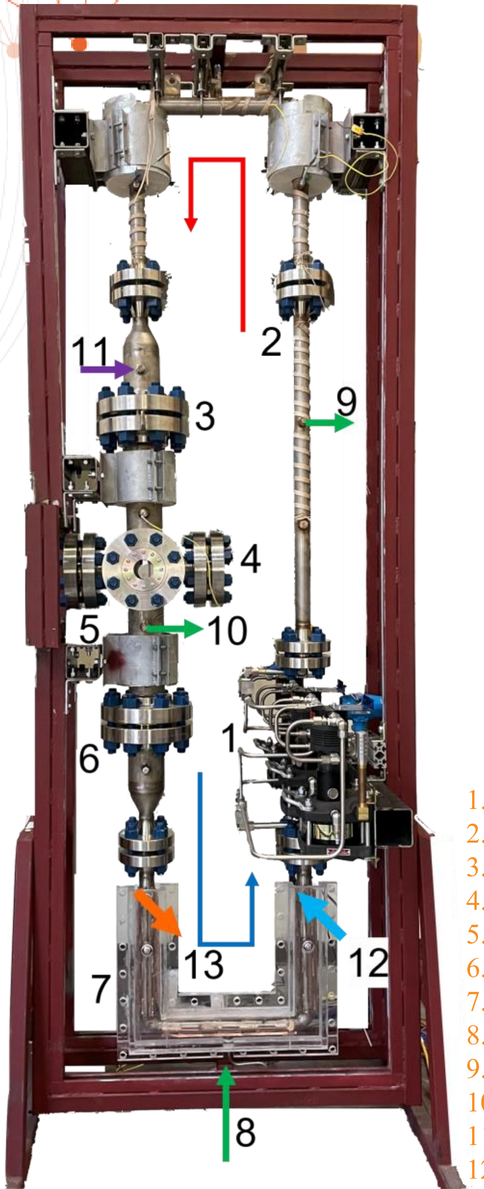

Experimental Planning	
Reynolds #	5,593-16,780
Geometry	Single Sphere, Over Helical Coil
Pressure	Atm-1,000 psig
Test Article Heating/Cooling (Isothermal - Nonisothermal)	ΔT = 0°C, 25°C, 50°C, 100°C ($\Delta T = T_{surface} - T_{helium}$)

1. Gas Boosters
2. Orifice Flowmeter
3. Flow Conditioner
4. Test Article Mounting/Feedthroughs
5. Quartz Sight Glass Windows for Imaging
6. In-Line Filtration
7. Cooling Jacket
8. Gas Filling
9. Pressure Control Valve (PID)
10. Rapid Depressurization Valve
11. Liquid/Solid Aerosol Injection
12.-13. Cooling Jacket Water Inlet/Outlet

Atmospheric P/T Deposition Experiments

Purpose

- Investigate graphite deposition patterns
- Saturation times for model comparison,
- Onset and growth of sedimentation patterns,
- PIV measurements for deposition velocity.

Re	V (m/s)
4,000	0.681
5,000	0.852
7,500	1.277
10,000	1.703
15,000	2.555
20,000	3.407
30,000	5.110
60,000	10.220
88,000	15.01

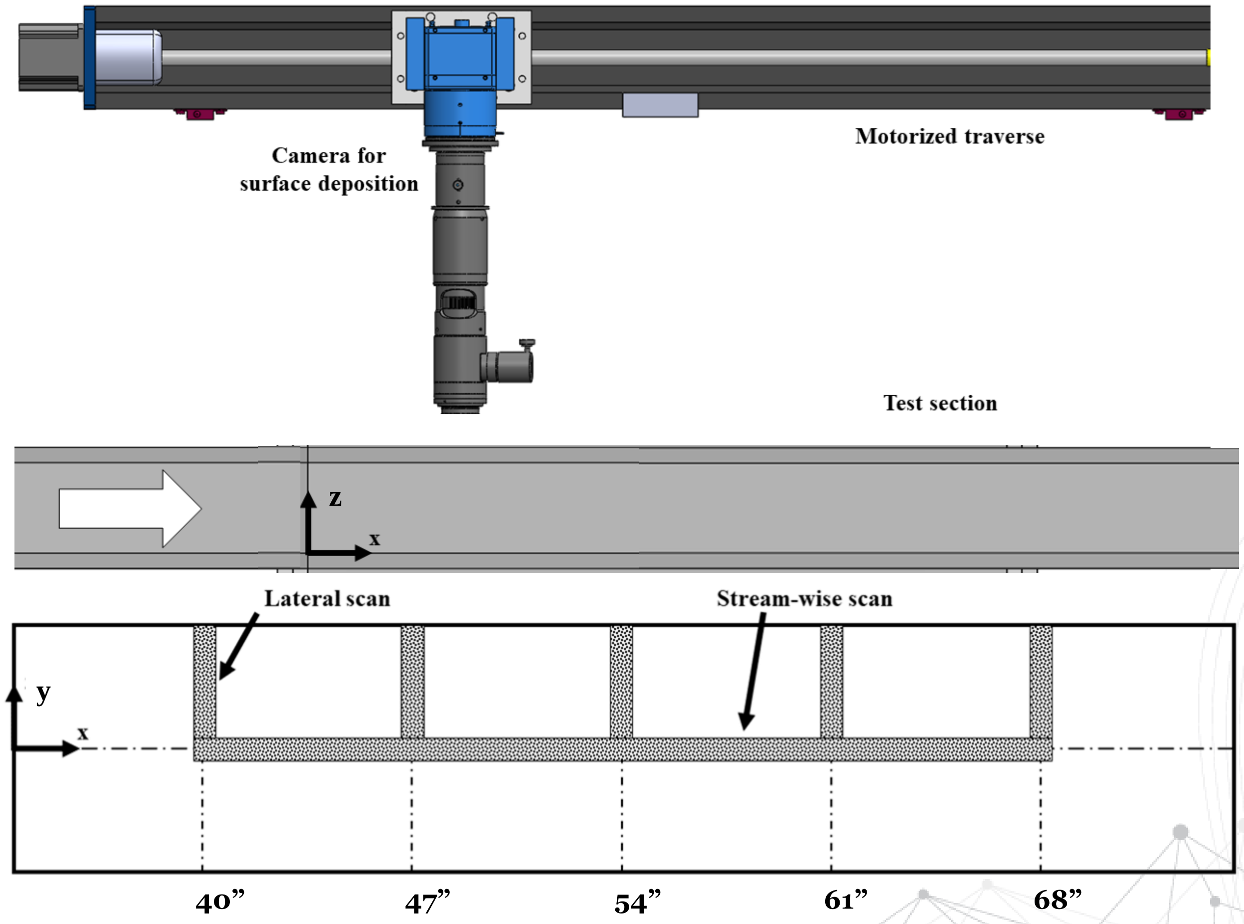

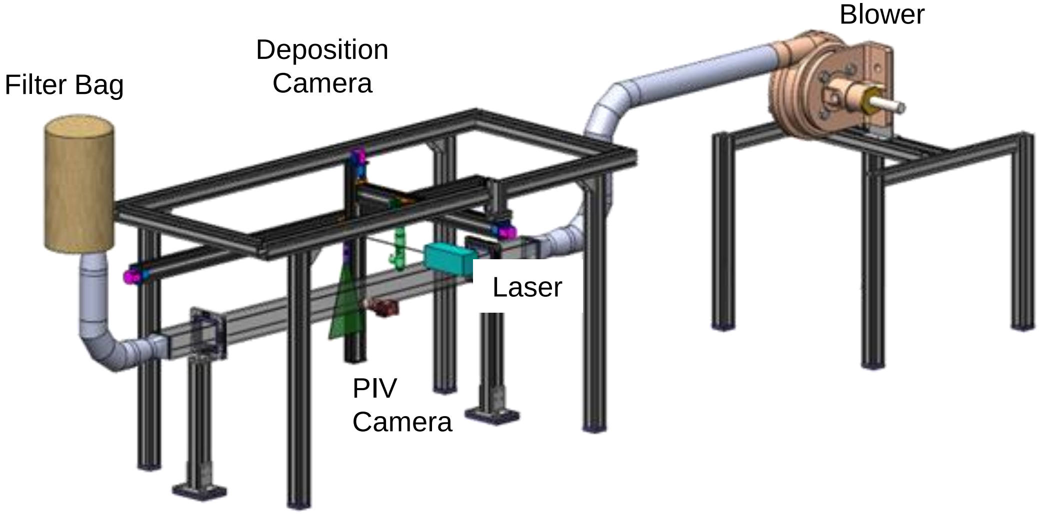

Long duration graphite deposition

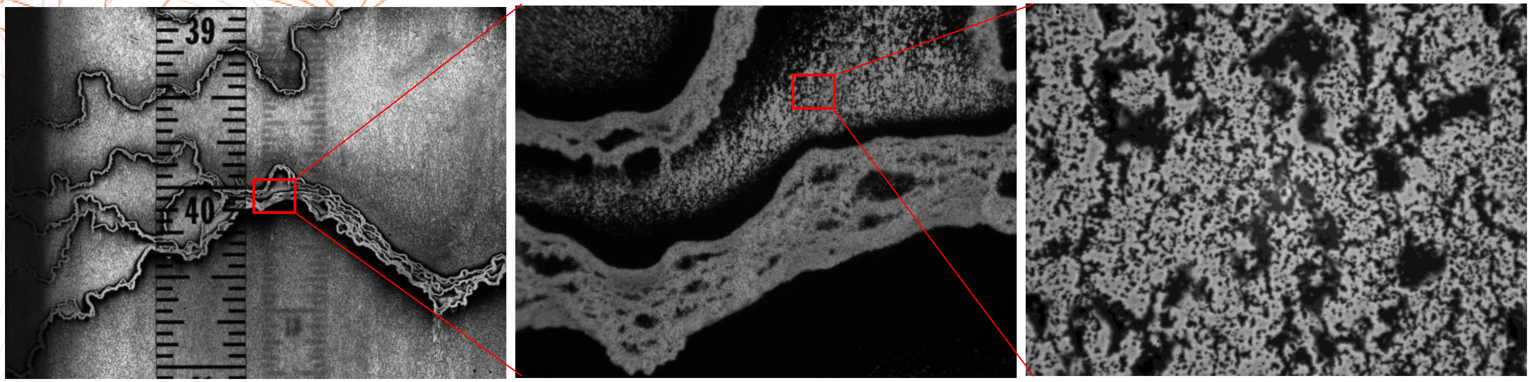

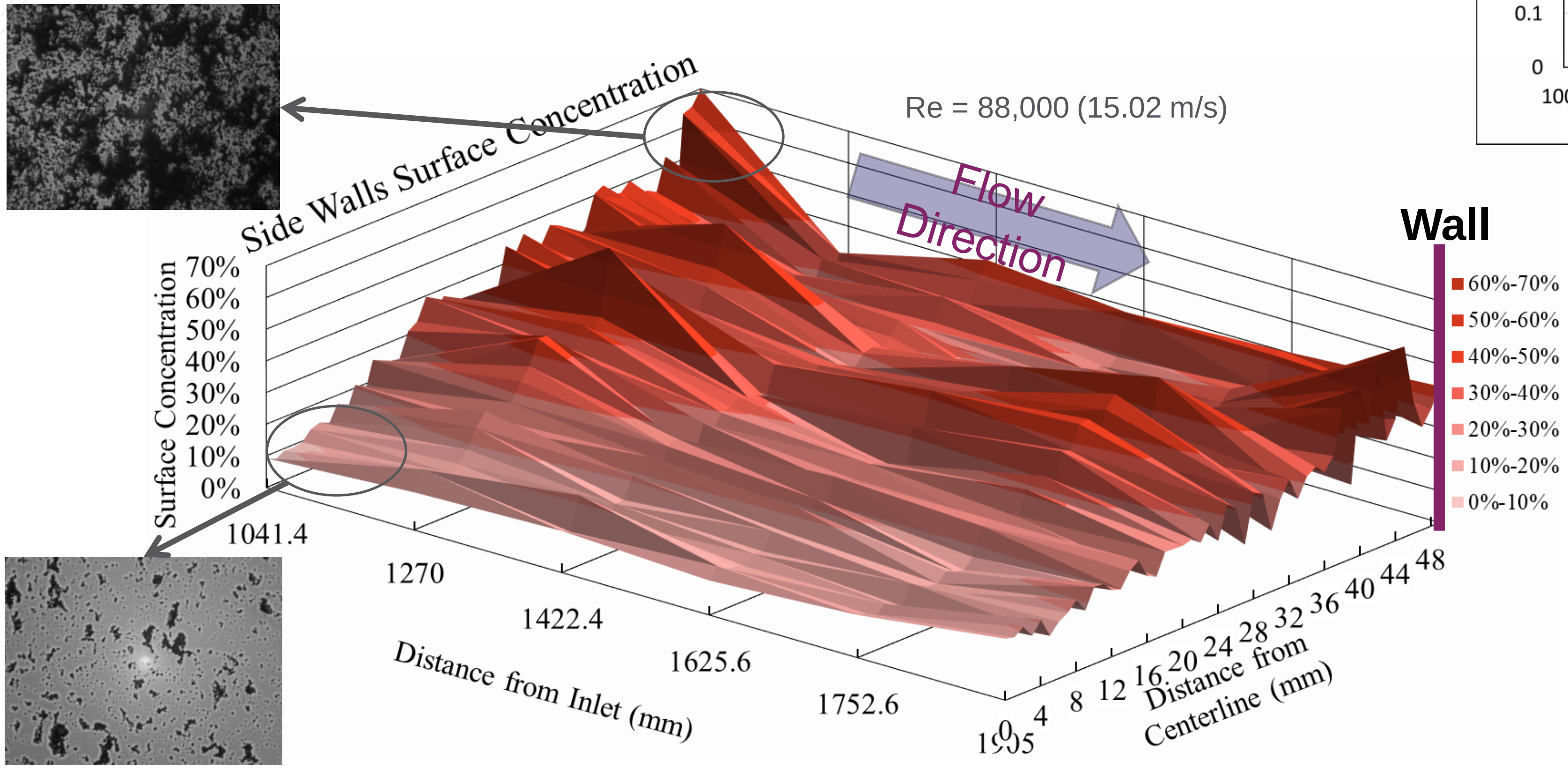

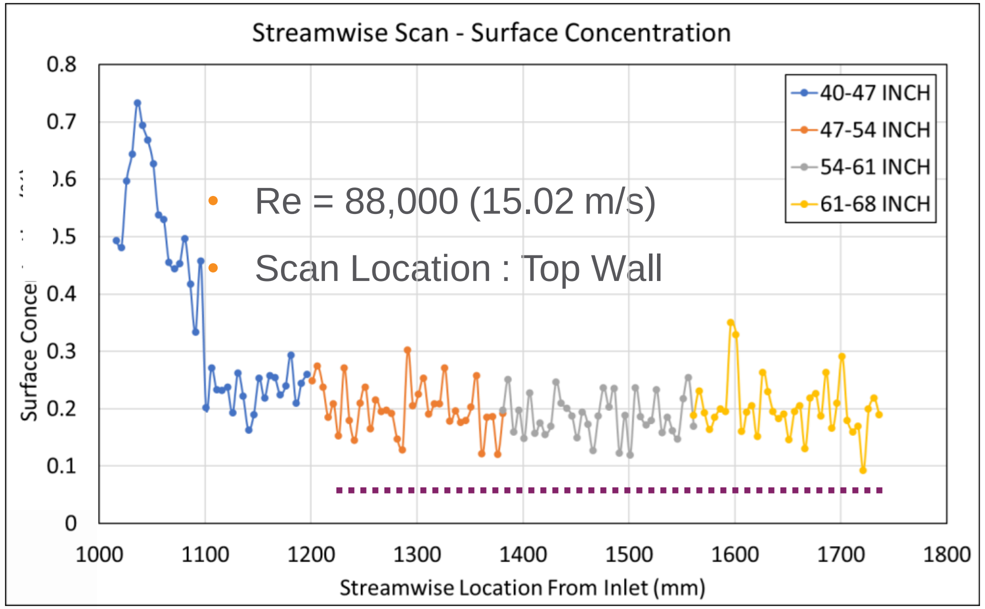

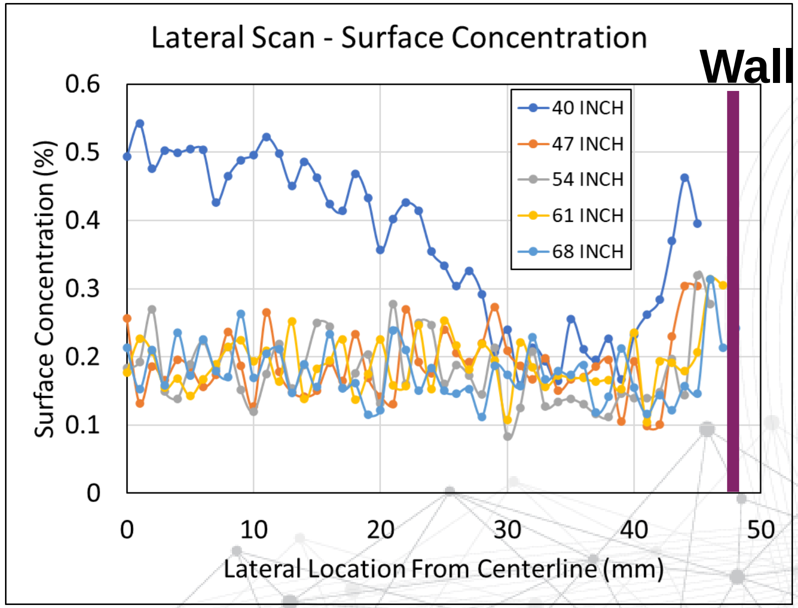

TEXAS A&M UNIVERSITY Engineering

Experimental Inputs to Model

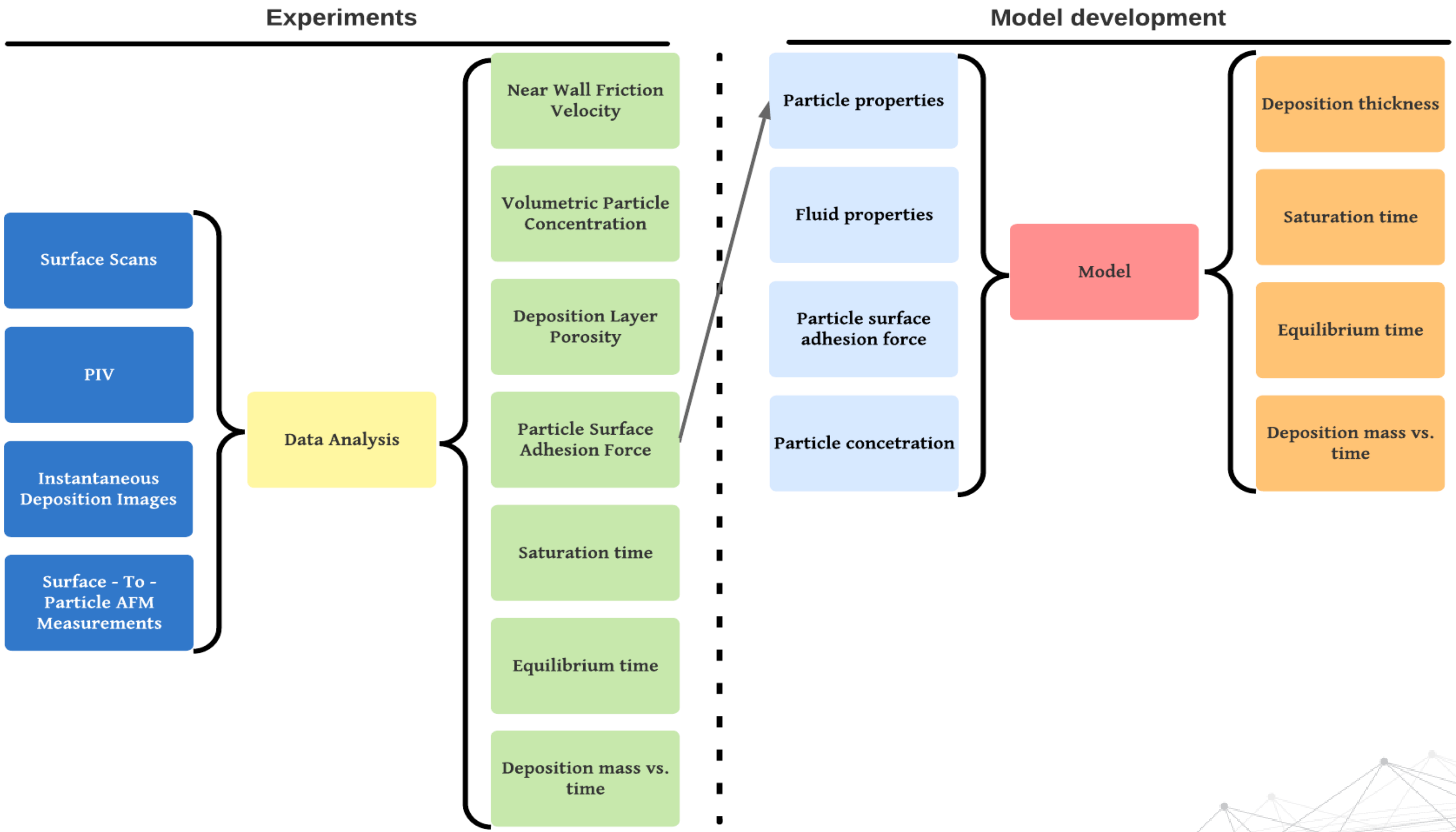

Model Development

- Smaller particles are harder to remove due to proportional forces (hydrodynamic torque, drag force, lift force, impact force) related to diameter.
- Higher free stream velocity increases impact force, making adhered particles easier to remove.
- Lower free stream velocity leads to smaller impact force, requiring higher critical shear velocity for particle removal.

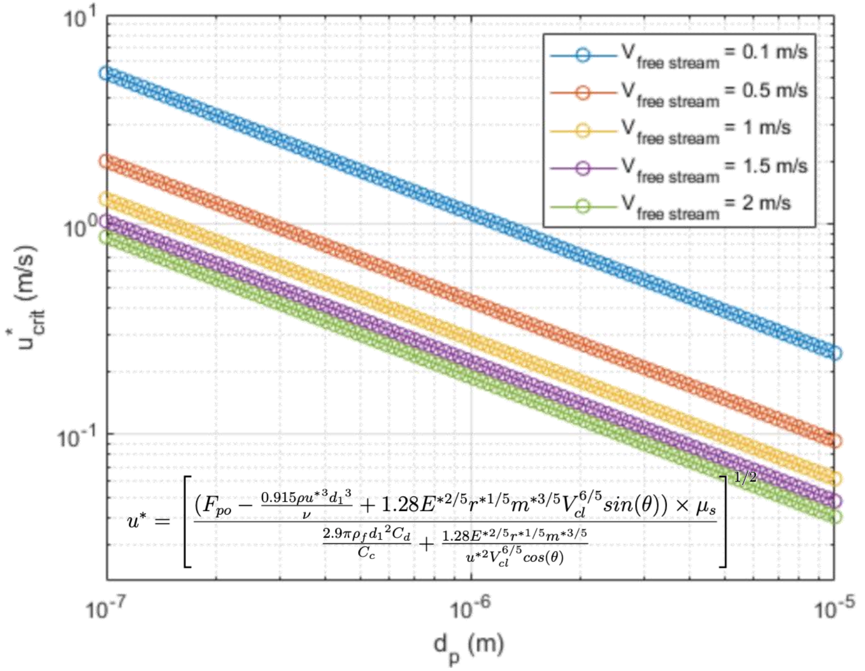

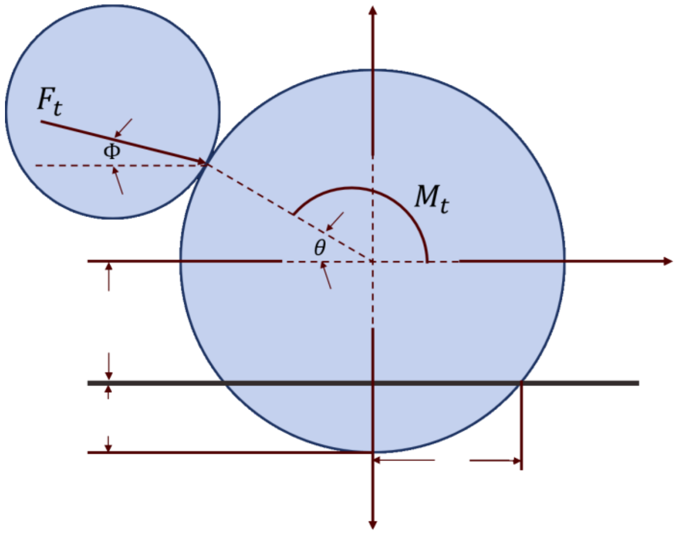

$$m(t) = \delta_c A(1 - \epsilon_{3D})\rho_{part}(1 - e^{-\frac{3t}{2t_{sat}}})$$

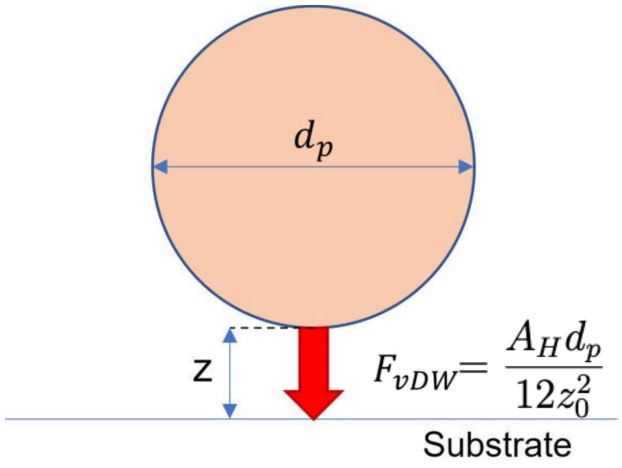

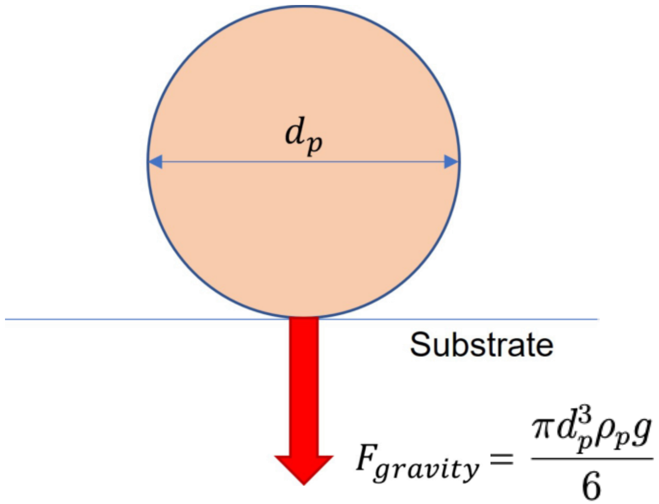

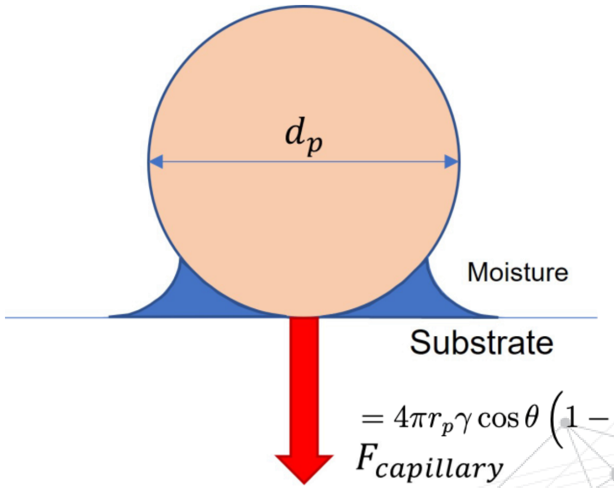

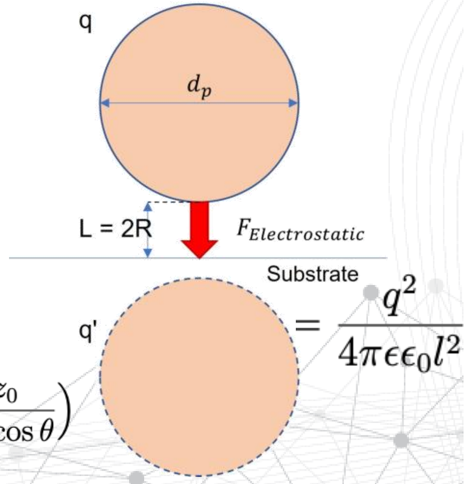

Numerical Validation

- ANSYS Fluent used to compute wall shear stresses for different Re numbers.
- Fully developed and turbulent before and after asymptotic deposition state.
- Critical shear velocity decreases with increasing free stream velocity, making it easier to remove adhered particles
- Proposed methodology accurately predicts the critical shear velocity and equilibrium deposition thickness, with a small difference compared to the results generated by computational fluid dynamics (CFD) simulations.

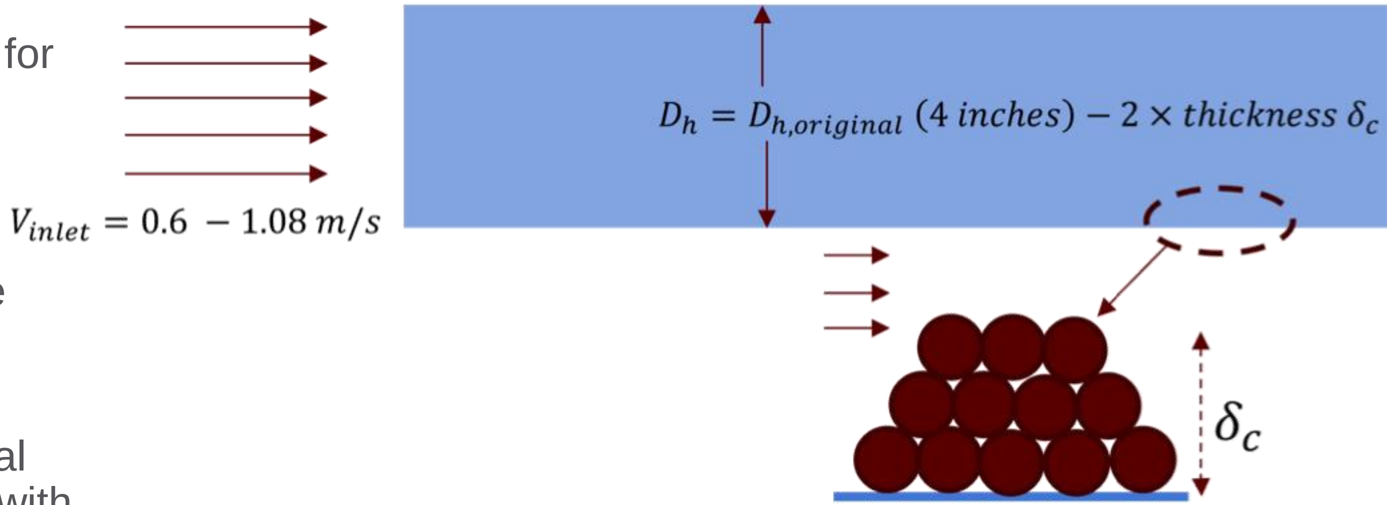

Inlet velocity (m/s)	δ_c (m)	u^*_{crit} (m/s) Analytical	Shear stress (Pa) CFD	u^* (m/s) CFD	Difference %
0.6	0.0214	0.07262	0.00767105	0.079133	8.23
0.7	0.0169	0.07210	0.00713851	0.076337	5.55
0.8	0.0124	0.07165	0.00679733	0.074491	3.81
0.9	0.008	0.07126	0.00649491	0.072815	2.13
1.0	0.0037	0.07091	0.00625974	0.071484	0.8
1.08	0.000217	0.07065	0.00614101	0.070803	0.22

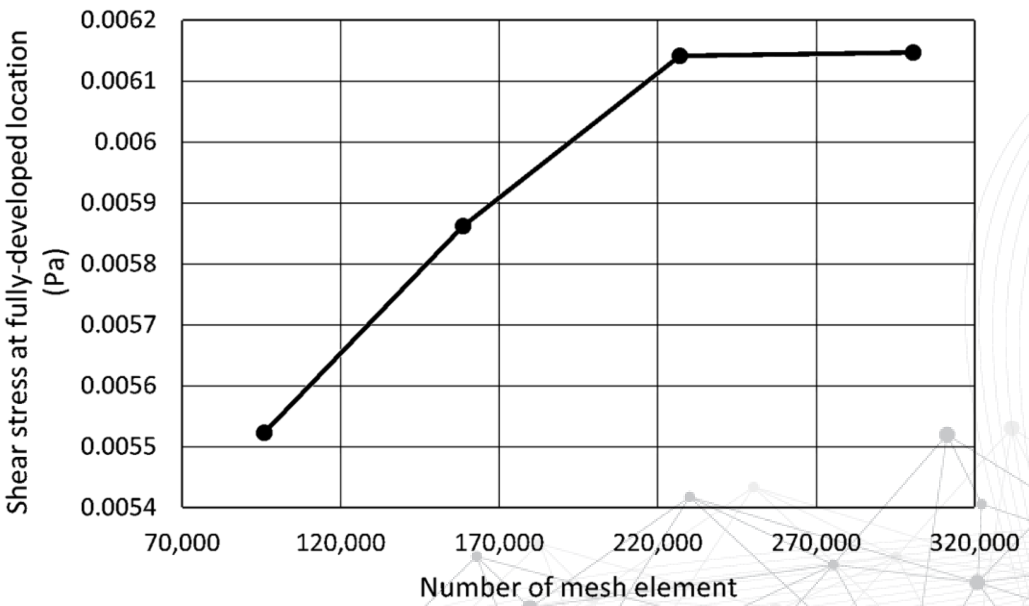

Nondimensionalization & Scaling Analysis

$$t_{sat}^{+} = \frac{t_{sat}U}{L_c} = \frac{135}{8}\left(\frac{1-\epsilon_{3D}}{u_d^{+}}\right)\left(\frac{\delta_c}{d_p}\right)\left(\frac{1}{Re_p}\right)\left(\frac{\Sigma m_f}{\Sigma m_p}\right)(Stk)$$

$$(u_d^{+})_M = (u_d^{+})_P \quad \left(\frac{\delta_c}{d_p}\right)_M = \left(\frac{\delta_c}{d_p}\right)_P$$

$$(Re_p)_M = (Re_p)_P \leftrightarrow \left(\frac{d_p u^*}{\nu_f}\right)_M = \left(\frac{d_p u^*}{\nu_f}\right)_P$$

$$(Re)_M = (Re)_P \leftrightarrow \left(\frac{\rho_f U D_h}{\mu_f}\right)_M = \left(\frac{\rho_f U D_h}{\mu_f}\right)_P$$

$$\left(\frac{\Sigma m_f}{\Sigma m_p}\right)_M = \left(\frac{\Sigma m_f}{\Sigma m_p}\right)_P \leftrightarrow \left(\frac{\rho_f}{C_0 m_p}\right)_M = \left(\frac{\rho_f}{C_0 m_p}\right)_P$$

$$(Sc)_M = (Sc)_P \leftrightarrow \left(\frac{\nu_f}{\frac{kT}{3\pi\mu_f d_p}}\right)_M = \left(\frac{\nu_f}{\frac{kT}{3\pi\mu_f d_p}}\right)_P$$

$$(\tau^{+})_M = (\tau^{+})_P \leftrightarrow \left(\frac{d_p^2 u^* \rho_p}{18\nu_f \rho_f}\right)_M = \left(\frac{d_p^2 u^* \rho_p}{18\nu_f \rho_f}\right)_P$$

$$(g^{+})_M = (g^{+})_P \leftrightarrow \left(\frac{\nu_f g}{u^*}\right)_M = \left(\frac{\nu_f g}{u^*}\right)_P$$

$$Sc = \frac{\nu_f}{\frac{kT}{3\pi\mu_f d_p}} \rightarrow d_p = \frac{SckT}{3\pi\mu_f\nu_f}$$

$$Re_p = \frac{d_p u^*}{\nu_f} \rightarrow u^* = \frac{Re_p \nu_f}{d_p}$$

$$u^* = \sqrt{\frac{f}{2}}U \rightarrow U = \frac{u^*}{\sqrt{\frac{f}{2}}}$$

$$Re = \frac{D_h U}{\nu_f} \rightarrow D_h = \frac{Re\nu_f}{U}$$

$$\tau^{+} = \frac{d_p^2 u^{*2}\rho_p}{18\nu_f^2\rho_f} \rightarrow \rho_p = \frac{\tau^{+}18\nu_f^2\rho_f}{d_p^2 u^{*2}}$$

$$\frac{\Sigma m_f}{\Sigma m_p} = \frac{\rho_f}{C_0 m_p} \rightarrow C_0 = \frac{\rho_f}{\frac{\Sigma m_f}{\Sigma m_p}\frac{4}{3}\pi\frac{d_p^3}{8}\rho_p}$$

Parametric Study

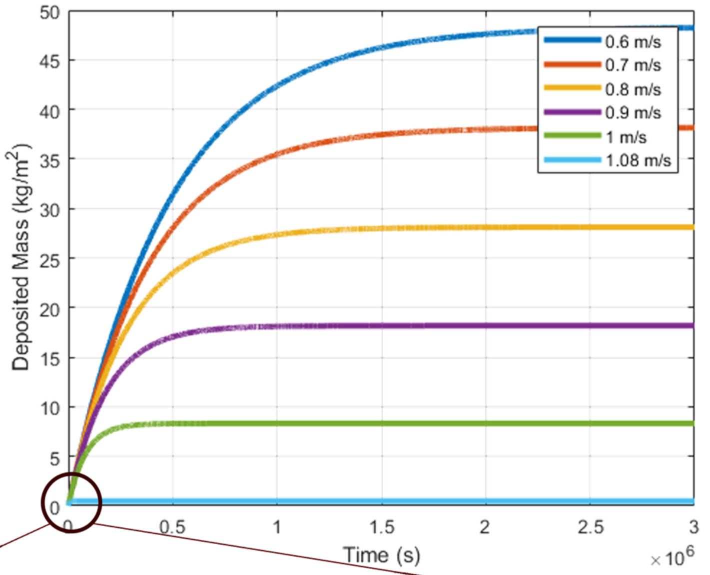

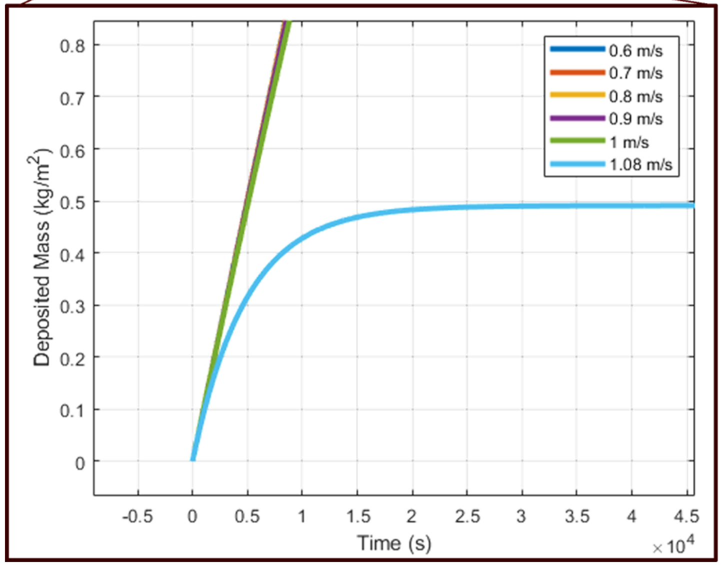

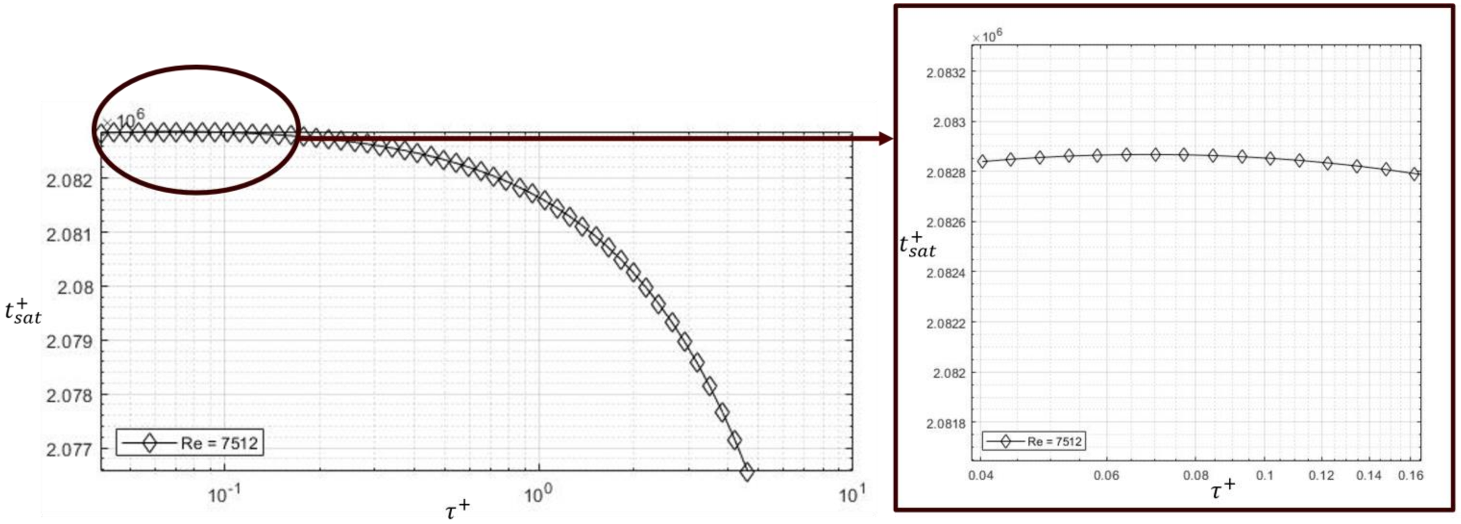

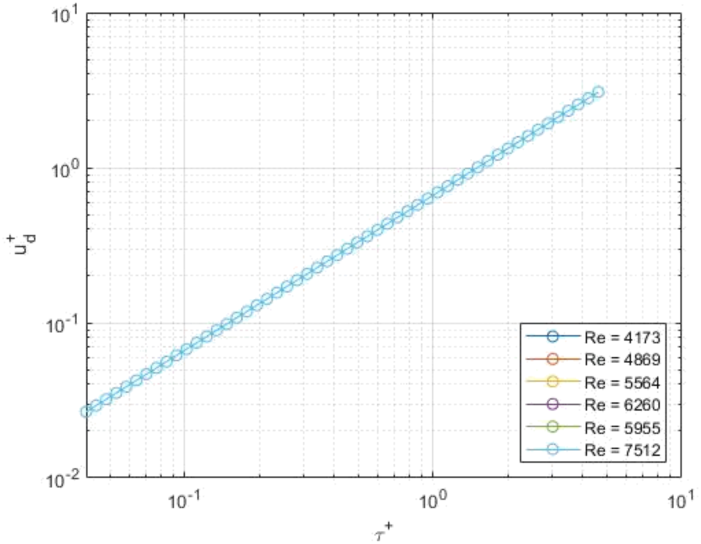

Inlet velocity (m/s)	Saturation time (hrs)	Equilibrium time (hrs)
0.6	199.05	610.50
0.7	157.22	482.19
0.8	115.85	355.31
0.9	74.88	229.67
1.0	34.28	105.13
1.08	2.02	6.20

Conclusions of Model Development, Numerical Validation, & Parametric Study

- Higher non-dimensional particle relaxation time -> Longer adjustment time to fluid streamlines -> More wall deposition likelihood -> Increased non-dimensional deposition velocity.
- Non-dimensional deposition velocity remains constant with increasing Re due to unaffected Brownian diffusion, eddy-impaction, and gravitational sedimentation.
- Increasing particle relaxation time at constant Re -> Increased deposition velocity -> Faster saturation and equilibrium time.
- Constant Re and particle relaxation time -> Higher fluid-to-particle mass ratio -> Decreased wall deposition -> Longer time to reach saturation.
- Higher inlet velocity at constant particle concentration -> Decreased saturation and equilibrium time.
- Increasing inlet velocity -> Decreased asymptotic deposited mass at fixed particle concentration -> Easier particle removal due to smaller critical shear velocity and fewer deposits.

- Journal article submitted and under review by Nuclear Engineering & Design.

Timeline

FY2022	Q1	Literature Review
FY2022	Q2	Model Development, Scaling, Nondimension-alization
FY2022	Q3	Experimental Planning
FY2022	Q4	Experimental Planning & Setup, CFD Pre-tests
FY2023	Q1	CFD Pre-tests, Experimental Setup
FY2023	Q2	Experimental Setup, Parametric study
FY2023	Q3	Plateout, Liftoff Experiments
FY2023	Q4	Plateout, Liftoff Experiments
FY2024	Q1	Experiment /Simulation Comparison with Analytical Model and Correlations
FY2024	Q2	Washoff Experiments, Uncertainty Analysis
FY2024	Q3	MELCOR Simulation Comparison, Correlation Development
FY2024	Q4	Final Report

Acknowledgements